Science & Technology Facilities Council

www.stfc.ac.uk

Solenoidal Focussing Internal Target Ring

C. T. Rogers*, STFC Rutherford Appleton Laboratory,

*chris.rogers@stfc.ac.uk

Internal Target Concept

In conventional accelerator-driven proton targets, protons are accelerated to high energy and deposited onto a target. Secondary particles are produced for users and any remaining protons are captured on a beam dump.

In so-called `internal target schemes', protons are accelerated to high energy and passed through a thin target that sits within a storage ring. The protons are recirculated through the ring, any lost energy being replaced by RF cavities, enabling many passes through the same target.

The ionisation cooling effect limits the amount of emittance growth that occurs upon passing through the target. Emittance growth due to scattering in the target is offset by emittance reduction due to the ionisation of atomic electrons, resulting in a stable equilibrium emittance.

Previous studies have used FFAG-type rings to accommodate the high emittances characteristic of internal target arrangements. FFAGs have excellent momentum acceptance and transverse acceptance, making them ideal candidates for such an arrangement. Solenoid rings have been studied extensively by the muon collider community for the purpose of ionisation cooling of muons, precisely because they have high acceptances. In this paper we study the use of a solenoid ring for proton containment.

Ring Model

The magnetic field at a radius of 3.0 m is shown in fig. 1. In this ring, combined-function solenoids and dipoles provide simultaneous focussing and bending.

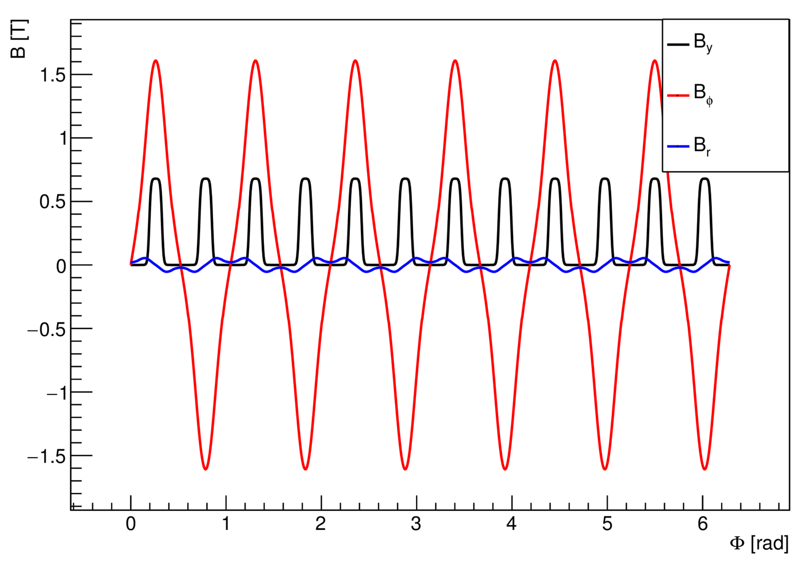

Fig.1: The magnetic field in the vertical, azimuthal and radial direction at a radius of 3.0 m is shown.

The ring shows good transverse acceptance. Eigenspace analysis was performed by calculating the one-turn transfer matrix numerically and then applying the Parzen algorithm to find the decoupled eigenspaces. The ring dynamic aperture in the two transverse eigenspaces is shown for the reference energy in fig. 2 and as a function of energy in fig. 3.

Performance

The performance was studied by injecting a pencil beam of 1000 protons at 11 MeV onto the reference trajectory. The protons were tracked until they were lost from the ring. The transverse emittance and energy spread of the beam are shown in fig. 4 and 5. The beam is observed to initially grow exponentially in transverse emittance. This is due to the scattering effect. An exponential fit was made to the emittance growth, showing that the emittance is convergent on an equilibrium value of about 0.24 mm.

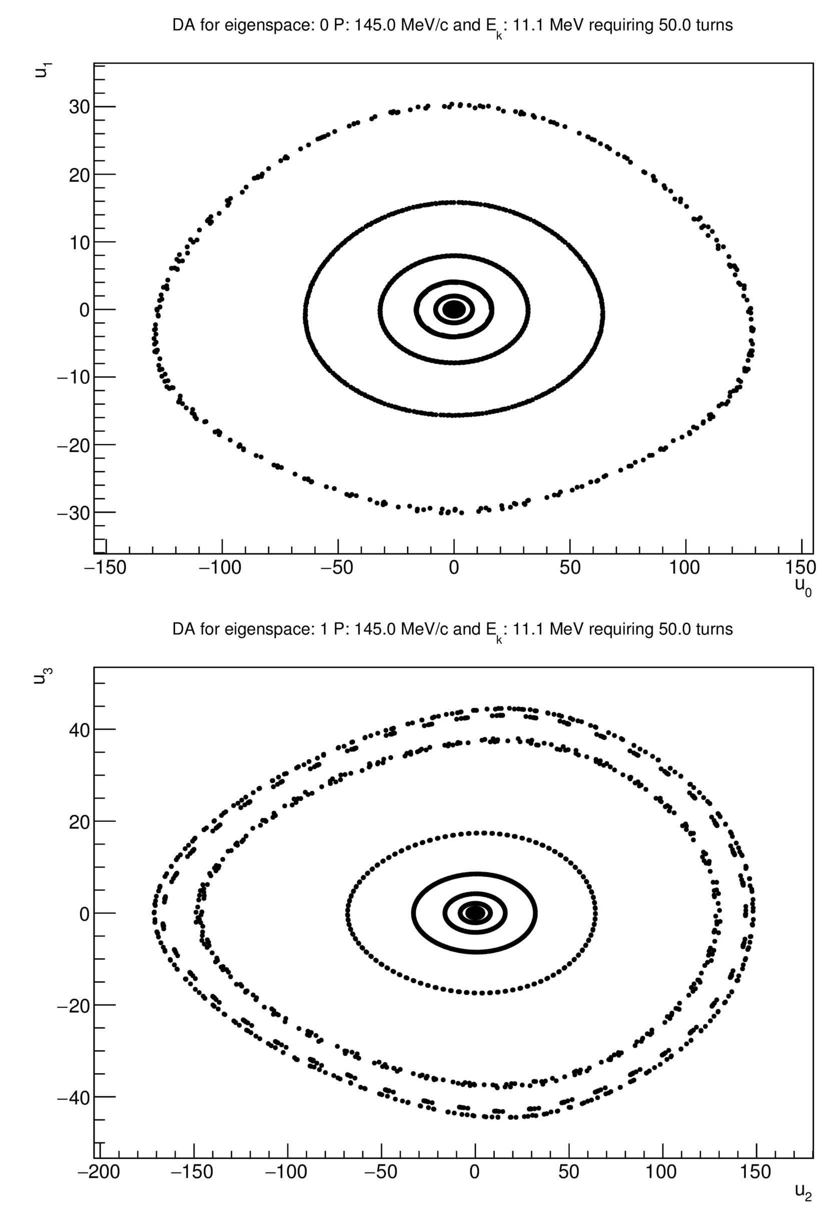

Fig.2: Evolution of particles in each dimensionless eigenspace through 50 turns (600 cells). The highest amplitude particles are on the dynamic aperture in (top) eigenspace 0 and (bottom) eigenspace 1.

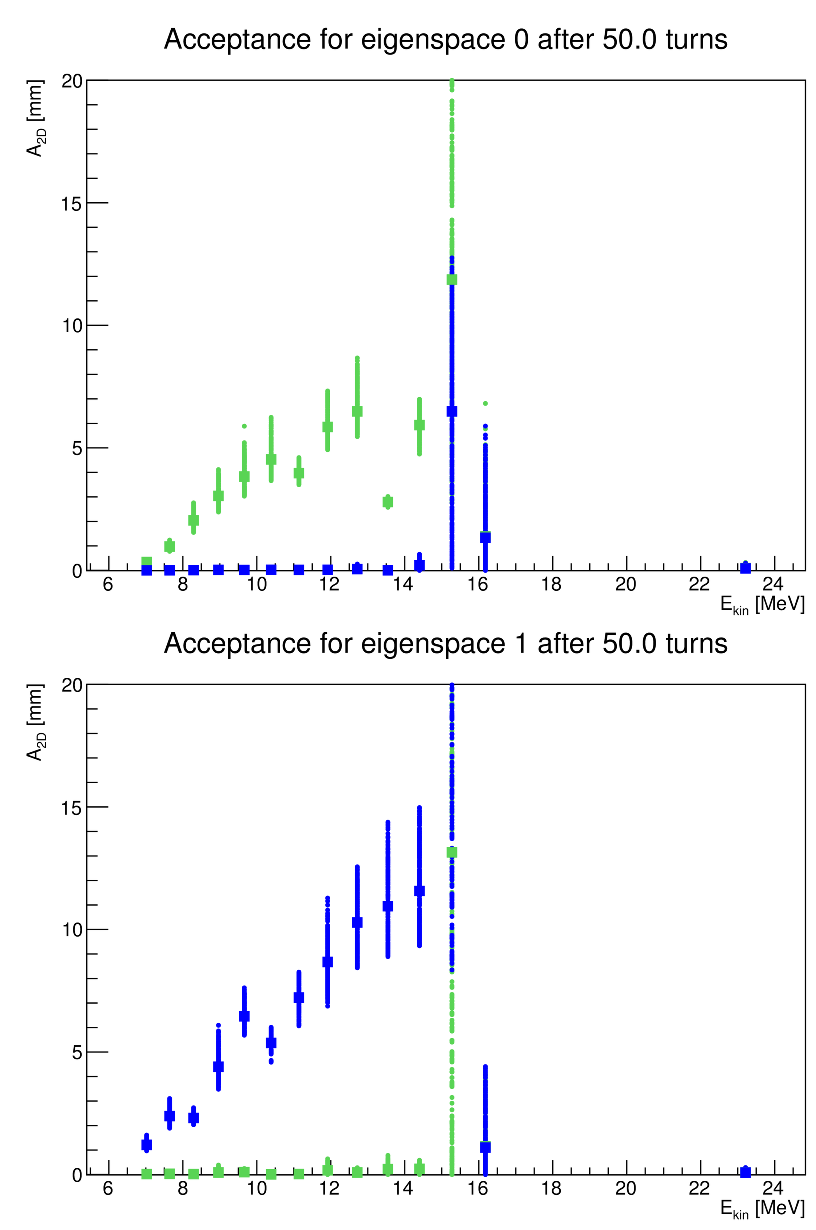

Fig.3: Amplitude of events at the dynamic aperture in the 0 (blue) and 1 (green) eigenspace as a function of energy. (Top) oscillations are excited in the 0 eigenspace and (bottom) oscillations are excited in the 1 eigenspace. Near to the 16 MeV stop-band, the eigenspaces are not well-decoupled.

Transmission is shown in fig. 6. Transverse losses become significant before the beam reaches the equilbrium emittance value. Beam lifetimes of a few microseconds are expected.

Longitudinal emittance spread is also induced in the beam due to the effects of energy straggling in the foil. Particles are seen to fall out of the RF bucket and this leads to longitudinal losses later in the cycle.

The total energy deposited by the protons is enhanced by the internal target system. Protons lose on average 48 MeV energy in the foil during the lifetime of the beam

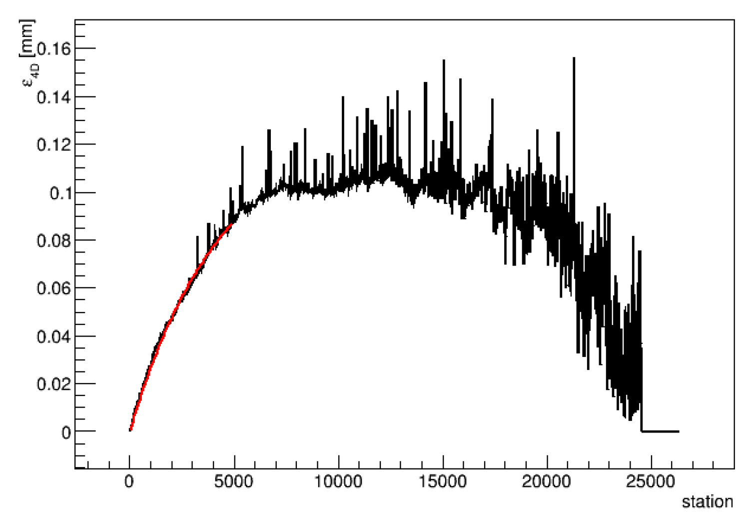

Fig.4: 4D transverse emittance as a function of number of cells traversed. The red line shows a fit of the form $A(1-e^{-n/n\_0})$

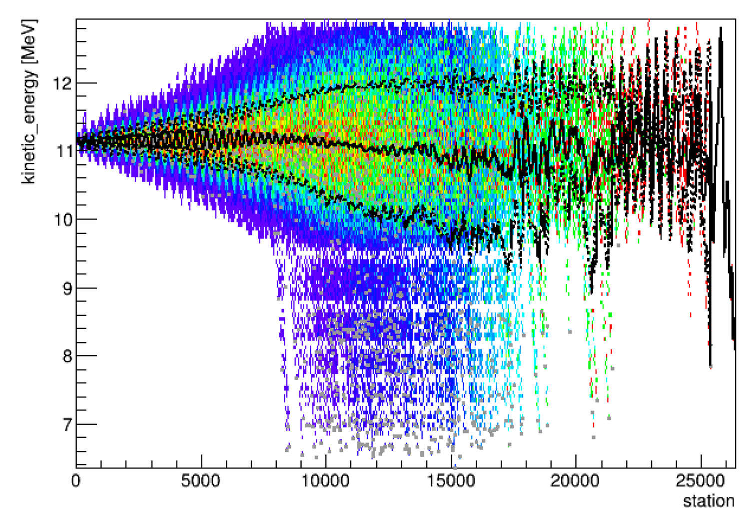

Fig.5: Kinetic energy as a function of number of cells. The black lines show the mean and +/- 1 standard deviation. Grey points mark the energy of protons in the cell immediately before they are lost.

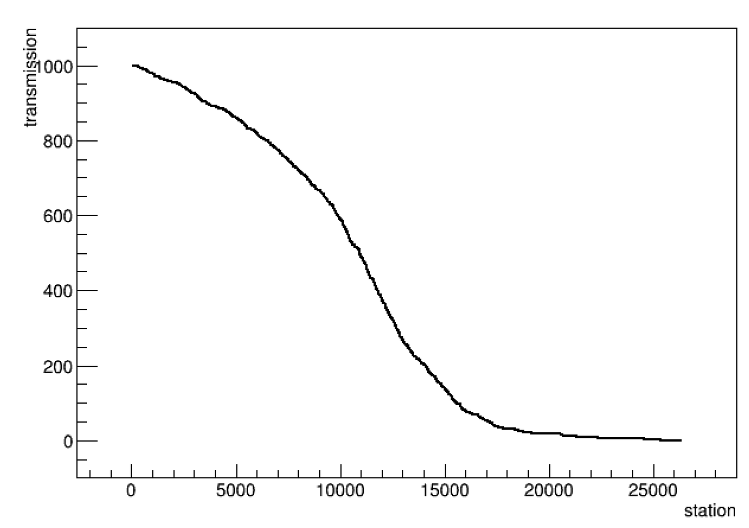

Fig.6: Transmission as a function of number of cells.

Conclusions

The internal target scheme provides a factor of almost 5 more energy deposited on the target per proton, compared to conventional target schemes. A concomitant improvement in secondary particle yield is expected. Simulated beam lifetime is a few milliseconds, which is sufficiently long that the machine could be operated in a continuous `top-up' mode given appropriate hardware. No injection scheme has been presented; charge-exchange injection would enable kicker-less injection.